Vol. 18, No. 3 (2019) 813-823
Revista Mexicana de Ingeniería Química

CONDUCTIVITY IMPROVEMENT OF TOPOLOGICAL INSULATORS OF Bi_2Se_3 BY THE P-N HETEROJUNCTION OF Bi_2Se_3/BiOCl

MEJORAMIENTO DE LA CONDUCTIVIDAD DE AISLANTES TOPOLÓGICOS DE Bi_2Se_3 POR LA HETEROUNIÓN P-N DE Bi_2Se_3/BiOCl

M. Evaristo-Vázquez[1], M.L. Hernández-Pichardo[1]*, E. Rodríguez-González[2]

[1]*Instituto Politécnico Nacional-Escuela Superior de Ingeniería Química e Industrias Extractivas, Laboratorio de Nanomateriales Sustentables, UPALM, 07738, México City, México.*
[2]*Instituto Politécnico Nacional- CICATA-Unidad Altamira, Tamaulipas 89600, México.*

Received: July 12, 2018; Accepted: August 20, 2018

Abstract

New Bi_2Se_3/BiOCl composites were synthesized with a p-n heterojunction by two synthesis methods: coprecipitation and hydrothermal. Likewise, some synthesis parameters were modified such as the stabilizing agent concentration (EDTA) and the synthesis temperature. The materials were characterized by X-ray diffraction (XRD), scanning electron microscopy (SEM), Raman spectroscopy and XPS spectroscopy. The electrical conductivity of the materials was determined by measuring the resistivity using the four point probe method. The results show that different growth mechanisms of the species are generated in the Bi_2Se_3/BiOCl composites, modifying the synthesis conditions. The morphologies and phases that are formed generate different electrical properties in these composites and the increase in the electrical conductivity of some samples can be attributed mainly to the formation of the stable p-n heterojunction between Bi_2Se_3 and BiOCl due to the generation of internal electric fields.

Keywords: Bi_2Se_3/BiOCl composites, topological insulators, p-n heterojunctions, electrical conductivity.

Resumen

Se sintetizaron nuevos compósitos de Bi_2Se_3/BiOCl con una heterounión p-n a través de dos métodos de síntesis: coprecipitación e hidrotérmico. Asimismo, se modificaron algunos parámetros de síntesis como la concentración del agente estabilizante (EDTA) y la temperatura de síntesis. Los materiales se caracterizaron por las técnicas de difracción de rayos X (DRX), microscopía electrónica de barrido (MEB), espectroscopía Raman y espectroscopía XPS. La conductividad eléctrica de los materiales se determinó mediante la medición de la resistividad empleando el método de cuatro puntas. Los resultados muestran que se generan mecanismos diferentes de crecimiento de las especies en los compósitos de Bi_2Se_3/BiOCl modificando las condiciones de síntesis. Las morfologías y fases que se forman generan diferentes propiedades eléctricas en estos materiales y el aumento en la conductividad eléctrica de algunas muestras se puede atribuir principalmente a la formación de la heterounión p-n estable entre el Bi_2Se_3 y el BiOCl debido a la generación de campos eléctricos internos.

Palabras clave: compósitos de Bi_2Se_3/BiOCl, aislantes topológicos, heterounión p-n, conductividad eléctrica.

1 Introduction

Topological insulators such as bismuth selenide (Bi_2Se_3) have recently attracted attention because these materials have different metallic states on their surface, which enable them to behave as insulators in the interior and as conductors on the surface (Liu *et al*., 2016). Recently, Bi_2Se_3 with characteristics of an n-type semiconductor has been extensively researched, since this material has a suitable band gap energy that can be used in several applications such as solar cells (Mane *et al*., 1999), thermoelectric materials (Kozma *et al*., 2015; Kadel *et al*., 2011) and photocatalysis (Gao *et al*., 2016).

On the other hand, it has also been found that the coupling of n-type semiconductors with p-type ones facilitates the separation of charge carriers from a p-type semiconductor, resulting in the generation of an internal electric field through the formation of a heterojunction, improving the conductivity of materials (Mehraj *et al*., 2016). Then, the development

* *Corresponding author. E-mail*: mhernandezp@ipn.mx
https://doi.org/10.24275/uam/izt/dcbi/revmexingquim/2019v18n3/Evaristo
issn-e: 2395-8472

of new materials with a p-n heterojunction such as Bi_2Se_3/BiOCl will allow the improvement of the metallic electron transport at the surface and its performance as field effect transistor, so these materials could have a suite of potential applications as thermoelectric materials (Kozma *et al*., 2015) as well as in nanoelectronics and spintronics (Zhu *et al*., 2013).

So far, new materials have been developed based on highly effective heterojunctions, including several materials based on bismuth (Mehraj *et al*., 2016; Chen *et al*., 2015; Gao *et al*., 2016). These materials have been synthesized in the form of powders or thin films by different synthesis methods such as CVD, pyrolytic spray, deposit by chemical bath and electrochemical deposit. However, typically, the nanomaterials synthesized by these methods exhibit low electrical conductivity, partially due to residues of chemical reagents in the bulk of the sample. Moreover, it has been found that the use of organic solvents (i. e., alkanethiol, alkylamine, tri-n-octylphosphine) to disperse the chemical precursors or stabilizers (dodecanethiol, ethylene-diamine-tetraacetic acid, thioglycolic acid) to form the desired morphology, inhibits the electrical properties of these materials (Kadel *et al*., 2011). Therefore, in this work, new Bi_2Se_3/BiOCl composites were prepared with a p-n heterojunction by two different chemical methods using water as a solvent, thus seeking to reduce the remains of chemical residues and increase their electrical conductivity.

2 Experimental part

Bi_2Se_3/BiOCl composites were synthesized by two different methods: coprecipitation (COP) and hydrothermal (HT) from bismuth chloride ($BiCl_3$, 98%) and selenium tetrachloride ($SeCl_4$) using ethylenediaminetetraacetic acid (EDTA) as a chelating agent, all from Aldrich.

2.1 Synthesis of composites by the coprecipitation method

The samples were prepare using 1.1 g of $BiCl_3$, 1.1 g of $SeCl_4$ and different amounts, from 0.33 to 0.99 g of EDTA. The precursors and the chelating agent were mixed to form an aqueous solution which was placed on ultrasound for 10 min. Subsequently, the solution was stirred at room temperature for 1 h. Then, sodium hydroxide and 0.58 g of sodium borohydride were added and the mixture was stirred at 75 °C until the appearance of a precipitate. Finally, the precipitate was separated by decanting, washed and dried at 110 °C for 4 h.

2.2 Synthesis of composites by the hydrothermal method

Similarly to the above method, 1.1 g of $BiCl_3$, 1.1 g of $SeCl_4$ and different amounts, from 0.33 to 0.99 g of EDTA were mixed to form an aqueous solution that was placed on ultrasound for 10 min. Subsequently, the solution was stirred at room temperature for 1 h. Next, sodium hydroxide and 0.58 grams of sodium borohydride were added and the solution was placed in an autoclave at 120 °C for 9 h. Finally, the precipitate was decanted, washed and dried at 110 °C for 4 h.

2.3 Characterization of composites

The materials were characterized by X-ray diffraction (XRD), scanning electron microscopy (SEM), Raman spectroscopy and XPS spectroscopy. The XRD analyzes were carried out by using a diffractometer RIGAKU model Miniflex 600 with an X-ray tube with Cu radiation $K_\alpha(\lambda = 1.5418$ Å). The used power was of 40 kV and 15 mA with a step of 0.02 and a speed of 5°/min. The Raman spectroscopy analyzes were carried out using a HORIBA spectrometer Jobin Yvon equipped with a CCD detector using a 532-nm excitation laser. The XPS spectra were obtained in a K-Alpha equipment from Thermo Scientific, which has an Al K_α source and a monochromator. The general spectra were obtained by using step energy of 160 and 60 eV for the high resolution spectra. In the case of these samples, a load compensation system was used. Finally, the samples were studied by SEM using a Nova 200 Nanolab double-beam microscope, scanning electron beam emission field, with a resolution of 1.1 nm and a focused ion beam with a resolution of 1.7 nm.

2.4 Evaluation of the electrical conductivity of the composites

The measurements were made by the 4-point method from the value of the electrical resistivity. In a 4-pin equipment, a current (I) was applied between the end points and a potential difference between the two intermediate points ($\Delta V(a,b)$) was measured as shown in Fig 1.

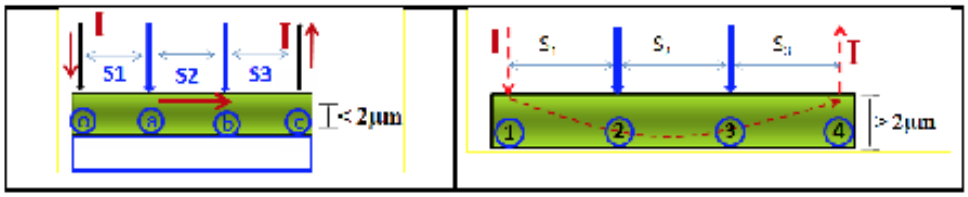

Fig 1. Schematic representation of the 4-point method principle for electrical resistivity.

For thin films ($d \leq 2\mu$m) deposited on a dielectric material, Fig. 1 (a), it can be assumed that all the current flows through the film. If, in addition, the tips are equally spaced apart, $S_1 = S_2 = S_3 = s$, then $a = s$ and $b = 2s$ and the film resistance [Ohm/frame] can be calculated as:

$$\rho_s = \frac{\rho}{t} = \frac{\pi}{\ln(2)} \frac{\Delta V(a,b)}{I} = 4.53236 \frac{\Delta V(a,b)}{I} \quad (1)$$

where the value for $\Delta V(a,b)/I$ is obtained by linear interpolation to the experimental data $\Delta V(a,b)$ vs. I recorded by the equipment.

In the case of coarse samples, thickness $d > 2\mu$m (Fig. 1(b)), the current that is injected through point 1 is evenly distributed in the material over a hemisphere of radius "r" centered at the point of contact that generates a current density (J).

$$J = \frac{I}{2\pi r^2} \quad (2)$$

Given the resistivity of the material (ρ_m), an electric field proportional to the current density $E = \rho_m J$ is induced, which generates a potential difference (ΔV) between separated points at different distance "r" from the contact point. Under these conditions, the potential difference between points 2 and 3 ($\Delta V_{3,2}$) is obtained by the expression:

$$\Delta V_{3,2} = \frac{\rho_m I}{2\pi} \left[\frac{1}{S_1} + \frac{1}{S_3} - \frac{1}{S_1 + S_2} - \frac{1}{S_3 + S_2} \right] \quad (3)$$

For the case where the tips are equally spaced apart, i.e. $S_1 = S_2 = S_3 = S$, then the potential difference is obtained from the relationship:

$$\Delta V_{3,2} = \frac{\rho_m I}{2\pi S} \quad (4)$$

And finally, the resistivity of the material is calculated as:

$$\rho_m = 2\pi S \times \frac{\Delta V_{3,2}}{I} [\text{ohm.cm}] \quad (5)$$

where the value of $\Delta V_{3,2}/I$, similar to the previous case, is obtained by linear interpolation to the experimental data $\Delta V_{3,2}$ vs. I given by the equipment.

In the case of the used equipment, the distance between points is S = 0.04 "= 0.1016 cm, so that the value of the resistance calculated by linear interpolation must be multiplied by the factor $2\pi S$ =0.638372 cm to obtain the resistivity of the material.

3 Results and discussion

3.1 *Effect of the synthesis method*

Bi_2Se_3/BiOCl composites were synthesized by using the coprecipitation and hydrothermal methods without organic solvents. The samples were labeled as BiSe-COP and BiSe-HT for the coprecipitation and hydrothermal methods, respectively. The results of their structural characterization and electrical conductivity are shown below.

3.1.1 *Characterization by X-ray diffraction (XRD)*

Figure 2 presents the diffraction patterns for the BiSe-COP and BiSe-HT samples. The presence of several phases in both systems is observed and it is highlighted that in the case of the sample synthesized by the hydrothermal method a higher amount of the rhombic phase of Bi_2Se_3 was obtained. This last phase was identified with the presence of peaks at 2θ = 18.6, 25.1, 29.4, 40.3, 43.8, and 47.9° (JCPDS card No. 00-033-0214). The presence of the bismuth oxychloride phase (BiOCl), identified with the peaks at 2θ = 12, 24.1, 27, 32.5, 33, 37, 46.4 and 49° (JCPDS card No. 06-0249), is also observed, which was formed from the reaction between the bismuth precursor ($BiCl_3$) and water, and which subsequently decomposes and reacts with $SeCl_4$ to form Bi_2Se_3.

The main Bi_2Se_3 peak at 2θ = 29.4 ° is framed in the blue box while the main BiOCl peaks are framed in the green box (Fig. 2). As it can be seen, Bi_2Se_3 is found in a higher proportion in the sample synthesized by the hydrothermal method (BiSe-HT).

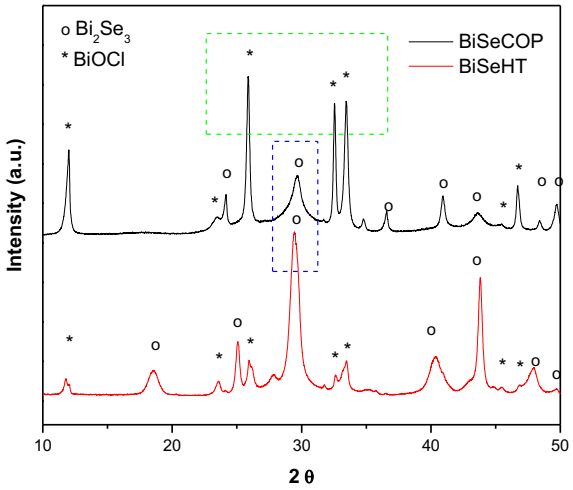

Fig. 2 Diffraction patterns of the BiSe-COP and BiSe-HT samples.

This may indicate that in the case of the BiSe-COP sample, the crystalline phase of the selenide was not formed due to the lowest synthesis temperature as well as the reaction time used in this method.

3.1.2 Characterization by Raman spectroscopy

In Figure 3, the Raman spectra obtained at different points of the BiSe-COP and BiSe-HT samples are presented. The measurements were made by using a laser λ = 532 nm. In these spectra, the bands representative of the formation of Bi_2Se_3 appeared at approximately 68, 125, 170 and 250 cm^{-1}, mainly in the sample synthesized by the hydrothermal method.

The bands at 125 and 170 cm^{-1} were assigned to the E_g^2 and A_{1g} vibrational modes of Bi_2Se_3, which are characteristic of this compound in the active modes in Raman (Zhang *et al.*, 2011). Likewise, in the case of the BiSe-COP sample, other bands are also observed at 140 and 198 cm^{-1}, which are attributed to the formation of BiOCl, also found by XRD. BiOCl has a tetragonal structure of the spatial group (D4h7); for this structure, the active modes in Raman are A_{1g}, B_{1g} and E_g (Xiong *et al.*, 2011). The spectra in Fig. 3.2 present an intense band at 140 cm^{-1} that was assigned to the internal Bi-Cl stretching mode A_{1g} and a weak band at 198 cm^{-1} that could be assigned to the E_g mode of the Bi-Cl bond. These results coincide with the results found by XRD and also corroborate a greater formation of Bi_2Se_3 obtained by the hydrothermal method.

3.1.3 Characterization by XPS spectroscopy

Figures 4 to 6 show X-ray photoelectron spectroscopy (XPS) high resolution spectra of the samples synthesized by the coprecipitation and hydrothermal methods. Figure 4 shows the comparison between the BiSe-COP and BiSe-HT spectra in the Se 3*d* and Bi 4*f* regions, respectively. In both samples, bands in coincident regions corresponding to the formation of Bi_2Se_3 are observed while it is clear that the BiSe-COP sample has wider bands that correspond to the formation of other compounds present in this sample, and that according to the results above, confirm the increased presence of bismuth oxychloride on the surface of this sample.

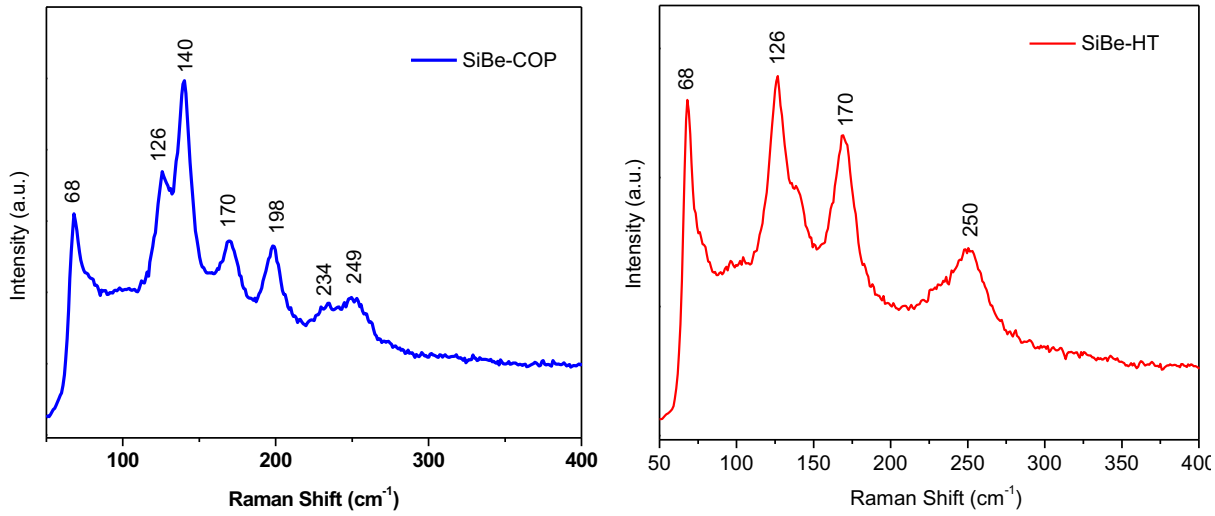

Fig. 3 Raman spectra in the region from 50 to 400 cm^{-1} of the BiSe-COP and BiSe-HT samples.

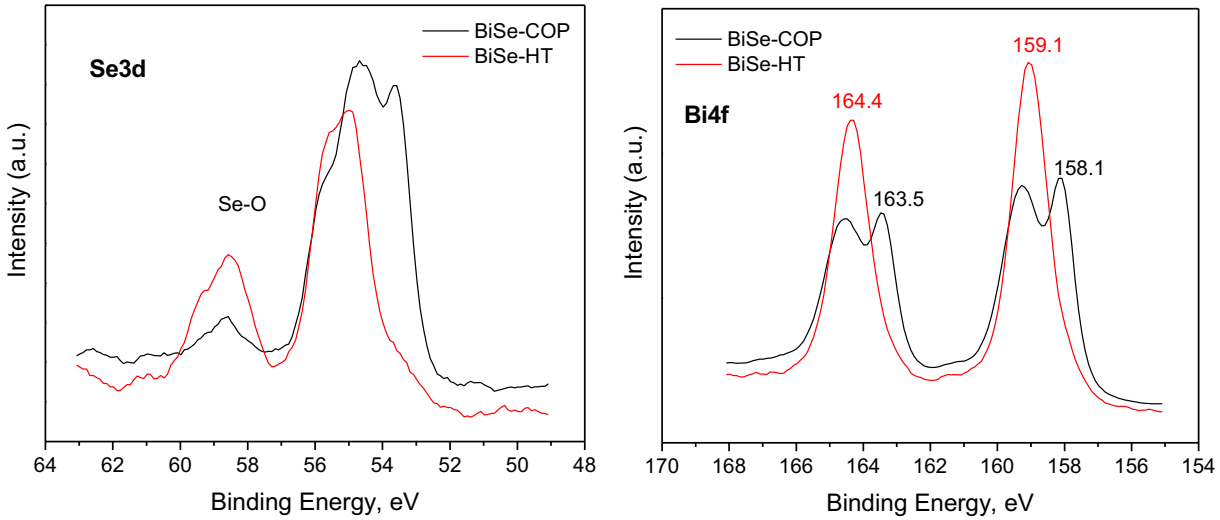

Fig. 4 High resolution XPS spectra in the Se 3d and Bi 4f regions of the BiSe-COP and BiSe-HT samples, respectively.

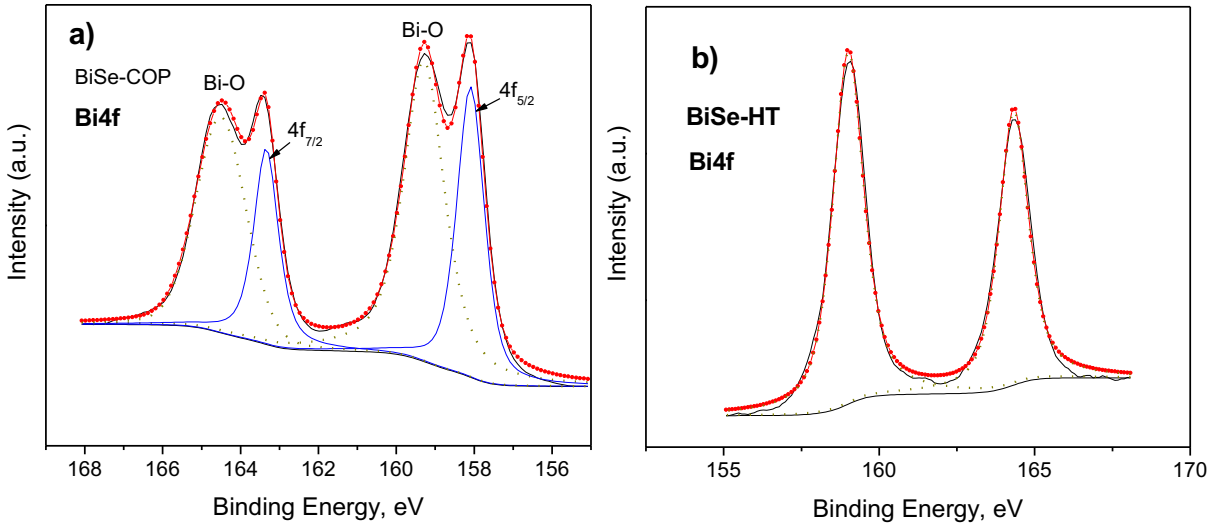

Fig. 5 Deconvolution of the XPS spectra in the Bi4f region of the samples: a) BiSe-COP and b) BiSe-HT.

In the Se 3*d* spectrum, an extra band between 58 and 60 eV that corresponds to the surface oxidation is also observed. Previous works have shown that air exposure caused the formation of an oxide layer on the Bi_2Se_3 surface (Zhou *et al*., 2016). In our case, strong selenium oxide (SeO_x) peaks are observed, mainly in the BiSe-HT sample, which suggests the surface oxidation of the Bi_2Se_3 samples produced by their exposure to the atmosphere. These results confirm that there is a higher formation of bismuth selenite in this sample. On the other hand, in the Bi 4*f* spectrum, the bands corresponding to the formation of Bi_2Se_3 can be seen at 164.4 and 159.1 eV while the bands corresponding to the formation of BiOCl are found at 163.5 and 158.1 eV (Tien *et al*., 2013).

To confirm these results, the deconvolution of the core level spectra of Bi 4*f*, for both samples, is shown in Figure 5. It is observed that both samples have a doublet at 164.4 and 159.1 eV that corresponds to the $4f_{5/2}$ and $4f_{7/2}$ doublets of Bi inside the crystalline Bi_2Se_3 lattice. However, the BiSe-COP sample (Fig. 5a) presents an extra doublet at 158.1 and 163.5 eV for Bi $4f_{5/2}$ and $4f_{7/2}$, respectively, which corresponds to the formation of BiOCl.

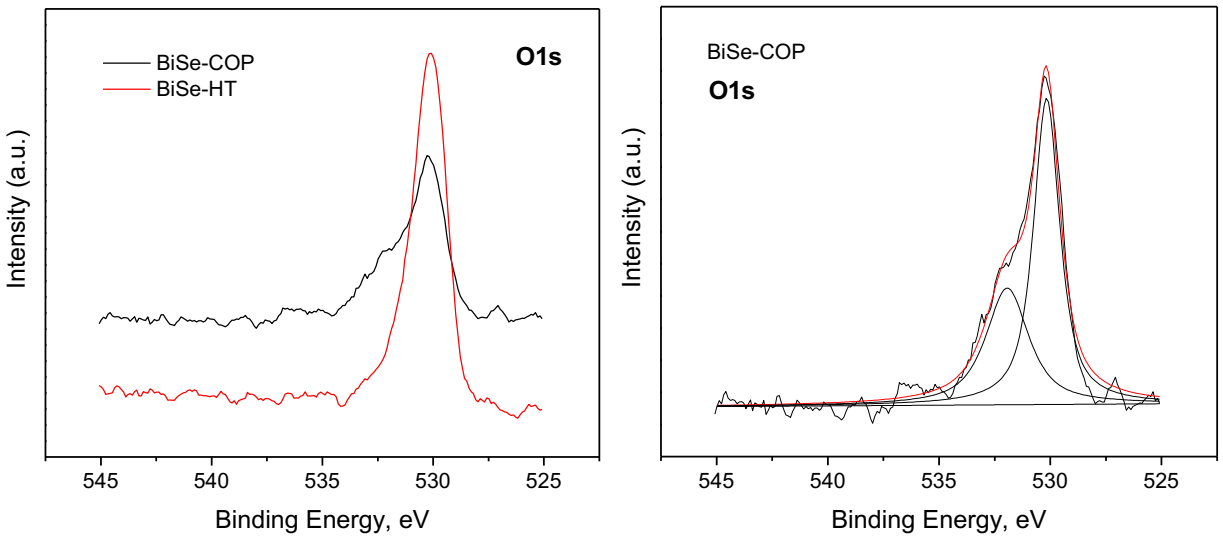

Fig. 6 High resolution XPS spectra in the O1s region of the BiSe-COP and BiSe-HT samples.

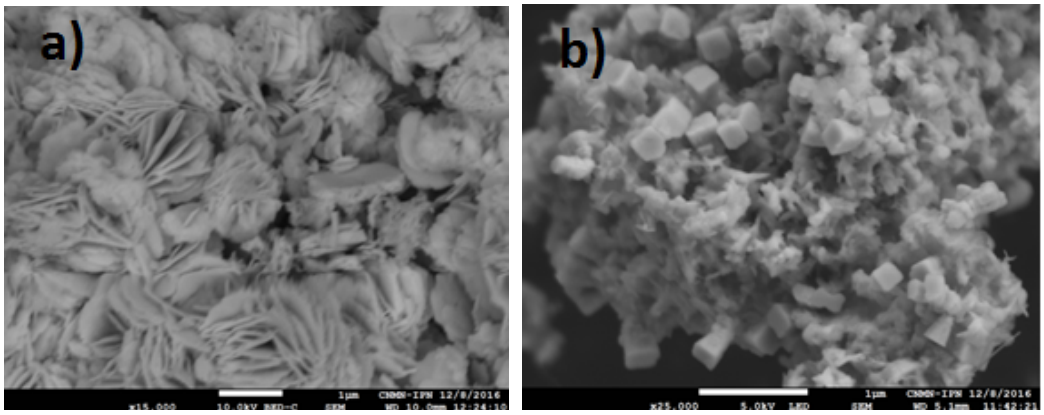

Fig. 7 SEM images of the samples synthesized by the methods: a) coprecipitation and b) hydrothermal.

The oxygen atoms bound to bismuth and chlorine in the structure give rise to a 1s peak of O near 532.1 eV (Fig. 6) while the BiSe-HT sample only presents an intense peak that corresponds to the surface oxidation of the Bi_2Se_3 samples.

The DRX, Raman and XPS results suggest that the formation mechanism of the Bi_2Se_3/BiOCl composites could be the decomposition of the $BiCl_3$ and $SeCl_4$ precursors to form BiOCl and the subsequent dissociation of the oxides to form bismuth selenide. (Keramidas *et al*., 1993, Smith *et al*., 1950).

3.1.4 Characterization by scanning electron microscopy (SEM)

Figure 7 presents the SEM images of the SiBe-COP and BiSe-HT samples. The SEM characterization of the composites shows that there are also morphological and structural differences in these materials. It is observed that the sample synthesized by the coprecipitation method has a relatively uniform flake-type morphology with different thicknesses while the sample synthesized by the hydrothermal method shows a more heterogeneous morphology with the formation of both more faceted particles and some cubes on its surface which are about 200 nm per side. It is also observe some differences in the texture and porosity of the samples, since the sample prepared by coprecipitation presents more homogeneous surface voids. The change in the morphology and texture of the sample synthesized by the hydrothermal method is due to the presence of the Bi_2Se_3 and BiOCl phases.

Table 1. Resistivity and electrical conductivity of Bi_2Se_3/BiOCl samples.

Synthesis Method	Thickness (mm)	Resistance (Ω)	Resistivity (Ω.cm)	Conductivity (S.cm)
Coprecipitation	0.41	7392 ± 12	4719	2.1×10^{-4}
Hidrothermal	0.4	2.8 ± 0.1	1.79	0.5586

Table 2. Effect of the synthesis temperature on the resistivity and electrical conductivity of Bi_2Se_3/BiOCl samples.

Sample	Synthesis Temperature (°C)	Resistance (Ω)	Resistivity (Ω.cm)	Conductivity (S.cm)
BiSe-0.33-100	100	5586.01	3565.95	0.0003
BiSe-0.33-200	200	5.62	3.59	0.28
BiSe-0.33-300	300	464.2	296.33	0.003

3.1.5 Evaluation of electrical conductivity by resistivity measurements

Table 1 shows the resistivity results for the samples prepared by both methods. For these measurements, powders were pressed at 10 tons and tablets were formed with a diameter of approximately 15 mm and thickness of approximately 0.4 mm. According to the previous results, it was determined that the sample synthesized by the hydrothermal method had better electrical conductivity results; thus, a study of the effect of temperature and EDTA content was carried out by using this method.

3.2 Effect of synthesis temperature

According to the previous results, the method that gave the best results in terms of electrical conductivity was the hydrothermal one; so, this method was used to study the effect of the synthesis temperature and subsequently the EDTA content. The effect of the temperature was studied by using 100, 200 and 300 ºC, maintaining the EDTA molar ratio (0.33) from the hydrothermal method. The results of the structural characterization are shown in Figure 8.

From Figure 8, we can observe the presence of two phases: the rhombohedral phase of Bi_2Se_3 by means of the peaks at 2θ = 18.6, 25, 29.4, 41 and 43.7°, according to the card 00-033-0124, and the phase of bismuth oxychloride (BiOCl) is evidenced by the peaks at 2θ = 12, 27, 32.5, 33, 37, 46.4 and 49° (card 06-0249).

From the present phases, it is observed that as the synthesis temperature increases, a higher formation of Bi_2Se_3 and a lower concentration of BiOCl occur. This fact confirms that the formation mechanism of bismuth selenide needs the formation of bismuth oxychloride, which decomposes at higher temperatures and reacts with selenium species to form Bi_2Se_3. In addition, from the SEM images, it can be observed that the material undergoes a morphological transformation, which starts from a flower-shaped structure at low temperatures, which is modified to faceted plates from 200 nm to 1.5 μm in size, with different thicknesses at higher temperatures. The last one is the morphology reported for Bi_2Se_3 materials (Liu *et al*., 2016; Kadel *et al*., 2011).

Table 2 shows the resistivity results for these samples. It can be seen that the highest electrical conductivity was obtained with the sample synthesized at 200 °C. The features of this sample are in good agreement with its structural results (Fig. 8) in the presence of both phases. This result suggests the possible formation of a p-n heterojunction of Bi_2Se_3/BiOCl which facilitates the separation of charge carriers from a p-type semiconductor and results in the generation of an internal electric field that improves the conductive properties of the composite.

3.3 Effect of the stabilizing agent (EDTA) content

Below (Fig. 9) are the structural results of the variation of the stabilizing agent content (0, 0.33, 0.66 and 0.99 g of EDTA) at a constant temperature of 120 ºC. It is observed that the sample without EDTA presents the formation of particles with not defined morphologies and different sizes, although at this synthesis temperature it is possible to see the formation of faceted particles. As the content of EDTA increases, it is observed the formation of

two phases, one of them formed by solid polygonal columns and the other one with a more porous texture. From the characterizations by X-ray diffraction and SEM, it can be said that EDTA helps the reaction to progress faster, that is, by not introducing EDTA and having a relatively low synthesis temperature, the formation of bismuth selenide is minimal, however, when the proportion of EDTA increases, the presence of bismuth selenide in the sample is higher compared to bismuth oxychloride. Table 3 shows the EDTA effect on the conductivity of the composites.

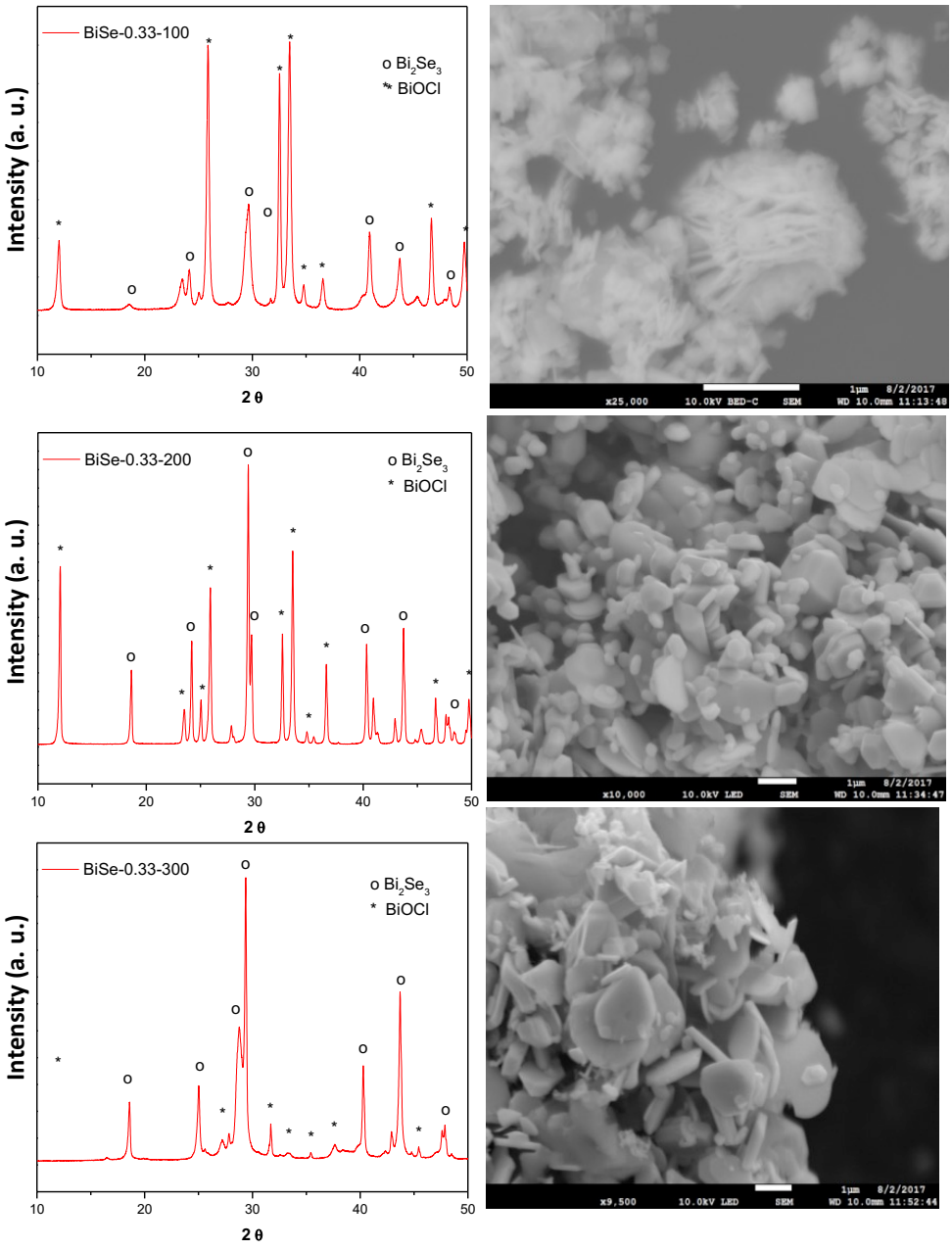

Fig. 8 Effect of the temperature: structural modifications of composites at 100, 200 and 300 ° C.

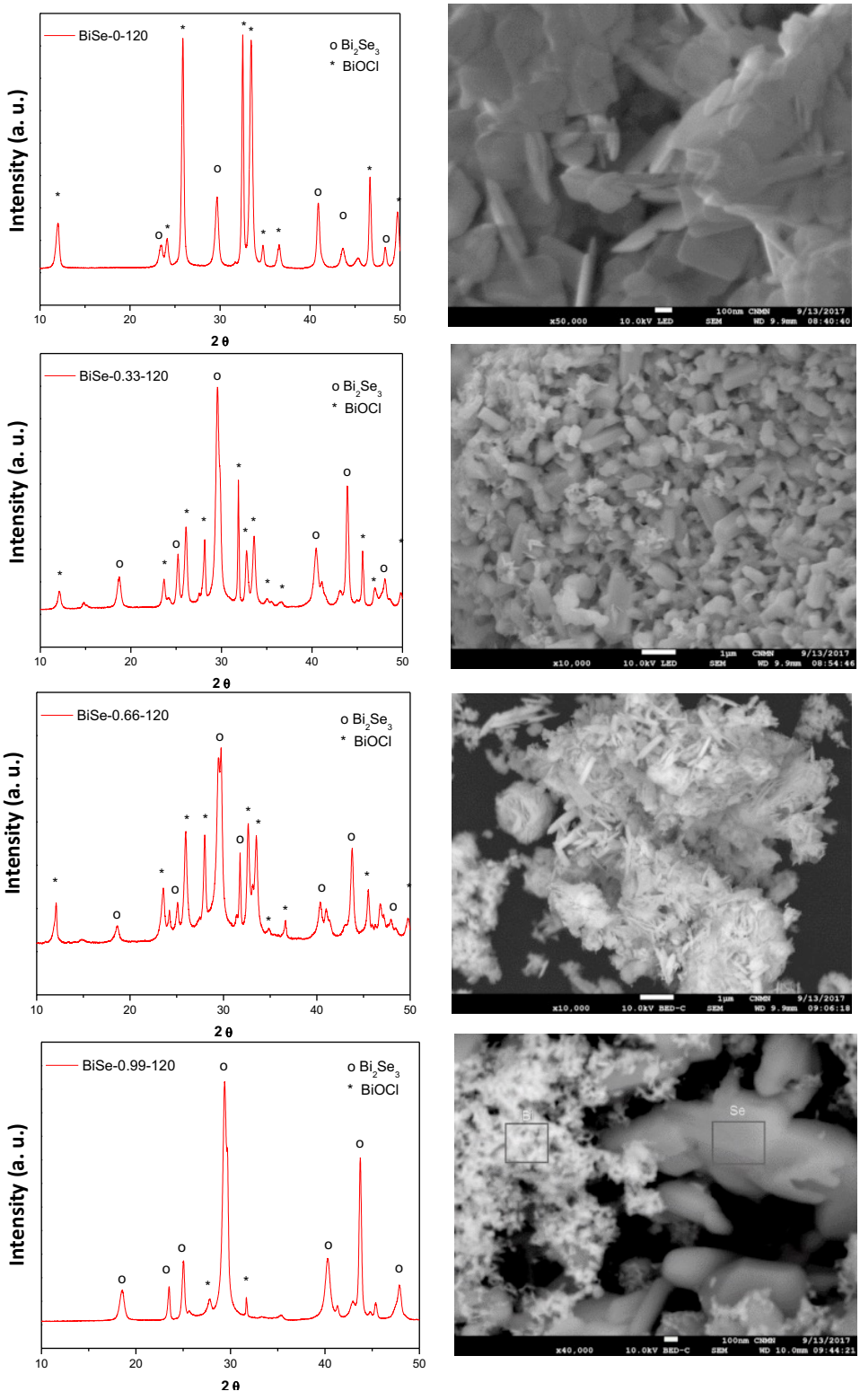

Fig. 9 Effect of the content of the stabilizing agent on the structure of the composites.

Table 3. Effect of variation of EDTA content.

Sample	EDTA (g)	Synthesis Temperature (°C)	Resistance (Ω)	Resistivity (Ω.cm)	Conductivity (S.cm)
BiSe-0-120	0	120	–	–	–
BiSe-0.33-120	0.33	120	31.97	20.41	0.05
BiSe-0.66-120	0.66	120	59.29	37.85	0.03
BiSe-0.99-120	0.99	120	7.53	4.81	0.21

As a summary, it was observed that from the hydrothermal method, different phases are obtained according to the synthesis temperature and the EDTA content. The main observed phases were bismuth selenide (Bi_2Se_3) and bismuth oxychloride (BiOCl). The sample with the highest conductivity was BiSe-0.33-200, followed by the BiSe-0.99-120 sample (0.28 and 0.21 S-cm^{-1}, respectively). The characterization results of these samples indicate that temperature is the main factor in the formation of these composites. Higher temperature leads to higher purity of the bismuth selenide, but a higher value of electrical conductivity is obtained when both phases are present. This may be due to the formation of a heterojunction, that is, a union of two materials with a different band gap that facilitates the flow of electrons, easing conductivity in these materials.

Conclusions

Bi_2Se_3/BiOCl composites were synthesized by using different preparation methods (coprecipitation and hydrothermal) under different synthesis conditions (temperature and EDTA content). It was observed that different mechanisms and morphologies of Bi_2Se_3 species were generated by the different methods. These features generated different electrical properties in these systems, being the samples prepared by the hydrothermal method the ones that had the highest electrical conductivity.

According to the results, both methods generated two phases, Bi_2Se_3 and BiOCl, however, the hydrothermal method favored the formation of Bi_2Se_3 due to the more severe conditions used in this method. It was also found that the effect that had greater influence on the formation of the phases was the temperature, the higher the temperature, the greater the amount of Bi_2Se_3 was observed, however, an increase in the electrical conductivity was obtained when both phases were present. These results may be due to the formation of a heterojunction that facilitates the flow of electrons, increasing the conductivity in these materials, which was indirectly observed by the decrease in resistivity. This result suggests the possible formation of a p-n heterojunction of Bi_2Se_3/BiOCl that facilitated the separation of charge carriers from a p-type semiconductor, resulting in the generation of an internal electric field and in the improvement of the composite conductive properties. The best sample was BiSe-0.33-200, which was synthesized by the hydrothermal method and prepared with a low EDTA content and at an intermediate temperature of 200 ºC.

Acknowledgements

The authors thank the Instituto Politécnico Nacional for financing this work through the Multidisciplinary Project "Preparation of Materials for Thermoelectric Applications", MD 20161767, projects SIP-20170399 and SIP-20170424.

References

Chen, Y., Liu, B., Chen, J., Chen, D., Yan, X., Xiao, W., Ge, L., Tu, M., Wang, Q., Wang, Z. (2015). Synthesis of BiOI/Bi@CNFs heteroarchitecture and its visible light photocatalytic properties. *Material Letters 161*, 289-293.

Gao, X., Huang, G., Gao, H., Pan, Ch., Wang, H., Yan, J., Liu, Y., Qiu, H., Ma, N., Gao, J. (2016). Facile fabrication of Bi_2S_3/SnS_2 heterojunction photocatalysts with efficient photocatalytic activity under visible light. *Journal of Alloys and Compounds 674*, 98-108.

Kadel, K., Kumari, L., Li, W.Z., Huang, J.Y., Provencio, P.P. (2011). Synthesis and thermoelectric properties of Bi_2Se_3 nanostructures. *Nanoscale Research Letters 6*, 2-7.

Keramidas, K.G., Voutsas, G. P., Rentzeperis, P. I. (1993). The crystal structure of BiOCl. *Zeitschrift für Kristallographie 205*, 35-40.

Kozma, A.A., Sabov, M.Y., Peresh, E.Y., Barchiy, I.E., Tsygyka, V.V. (2015). Thermoelectric properties of a eutectic $SnSe_2$-Bi_2Se_3 alloy. *Inorganic Materials 51*, 93-97.

Liu, X., Fang, Z., Zhang, Q., Huang, R., Lin, L., Ye, Ch., Ma, Ch., Zeng, J. (2016). Ethylenediaminetetraacetic acid-assisted synthesis of Bi_2Se_3 nanostructures with unique edge sites. *Nanoresearch 11*, 1-8.

Mane, R.S., Sankapal, B.R., Lokhande, C.D. (1999). Photoelectrochemical cells based on chemically deposited nanocrystalline Bi_2S_3 thin films. *Materials Chemical Physics 60*, 196-203.

Mehraj, O., Pirzada, B.M., Mir, N.A., Khan, M.Z., Sabir, S. (2016). A highly efficient visible-light-driven novel p-n junction Fe_2O_3/BiOI photocatalyst: Surface decoration of BiOI nanosheets with Fe_2O_3 nanoparticles. *Applied Surface Science 387*, 642-651.

Smith, G.B.L., Julius, J., (1950). Selenium (IV) oxychloride. *Inorganic Syntheses 3*, 130-137.

Tien, L., Lin, Y., Chen, S. (2013). Synthesis and characterization of Bi12O17Cl2 nanowires obtained by chlorination of α-Bi_2O_3 nanowires. *Materials Letters 113*, 30-33.

Xiong, J., Cheng, G., Li, G., Qin, F., Chen, R. (2011). Well-crystallized square-like 2D BiOCl nanoplates: mannitol-assisted hydrothermal synthesis and improved visible-light-driven photocatalytic performance. *RSC Advances 1*, 1542-1553.

Zhang, J., Peng, Z., Soni, A., Zhao, Y., Xiong, Y., Peng, B., Wang, J., Dresselhaus, M. S., Xiong, Q. (2011). Raman spectroscopy of few-quintuple layer topological insulator Bi_2Se_3 nanoplatelets. *Nano Letters 11*, 2407-2414.

Zhou, W., Zhu, H., Yarmoff, J. A. (2016). Termination of single-crystal Bi_2Se_3 surfaces prepared by various methods. *Physical Review B 94*, 195408-1-10.

Zhu, H., Richter, C. A., Zhao, E., Bonevich J.E., Kimes, W.A., Jang, H.J., Yuan, H., Li H., Arab, A., Kirillov, O., Maslar, J.E., Ioannou, D.E., Li, Q. (2013). Topological Insulator Bi_2Se_3 nanowire high performance field-effect transistors. *Scientific Reports 3*, 1-5.